Engineering Frequency-Time Quantum Correlation of Narrow-Band Biphotons from Cold Atoms

Young-Wook Cho,* Kwang-Kyoon Park, Jong-Chan Lee, and Yoon-Ho Kim†
Department of Physics, Pohang University of Science and Technology (POSTECH), Pohang 790-784, Korea
(Received 15 April 2014; published 5 August 2014)

The nonclassical photon pair, generated via a parametric process, is naturally endowed with a specific form of frequency-time quantum correlations. Here, we report complete control of frequency-time quantum correlations of narrow-band biphotons generated via spontaneous four-wave mixing in a cold atomic ensemble. We have experimentally confirmed the generation of frequency-anticorrelated, frequency-correlated, and frequency-uncorrelated narrow-band biphoton states, as well as verifying the strong nonclassicality of the correlations. Our work opens up new possibilities for engineering narrow-band entangled photons for various quantum optical and quantum information applications.

DOI: 10.1103/PhysRevLett.113.063602 PACS numbers: 42.50.Dv, 32.80.Qk, 42.50.Gy, 42.65.Lm

Photonic quantum states with nonclassical correlations play essential roles in quantum optics and quantum information. Engineering the nature of quantum correlations is, thus, an important problem, and considerable efforts have been paid to quantum state engineering in various photonic degrees of freedom, such as, polarization [1], photon number [2], orbital angular momentum [3], etc. Nonclassical biphotons generated via a parametric process, e.g., spontaneous parametric down-conversion and spontaneous four-wave mixing, are naturally endowed with specific forms of frequency-time quantum correlations. As illustrated in Fig. 1, the biphoton frequency-time correlation can be categorized as frequency anticorrelated, frequency uncorrelated, and frequency correlated. Because of the Fourier duality, the quantum correlation in the frequency domain can be reexpressed in the time domain but with the sign reversed: negative correlation in the frequency domain corresponds to the positive correlation in the time domain. The ability to manipulate the frequency-time correlation of the biphoton state is not only important in the fundamental study of continuous-variable quantum correlations, but also essential for a variety of quantum-based technologies, including quantum-enhanced clock synchronization [4,5], heralded generation of high-purity single-photon states [6–9], study of two-photon absorption processes [10], etc.

To date, research on engineering the biphoton frequency-time correlation has been mainly focused on spontaneous parametric down-conversion (SPDC) processes. While continuous-wave (cw) pumped SPDC in a bulk nonlinear crystal only generates frequency-anticorrelated biphoton states, it had been proposed that different biphoton correlations may be achieved by utilizing broadband pumping, dispersive properties of the nonlinear medium, and different phase matching conditions [11–13]. Recent experiments have demonstrated frequency-uncorrelated and frequency-correlated biphoton states, respectively, with a bulk [6,7,11] and a periodically poled nonlinear crystal [8,14,15]. Spontaneous four-wave mixing (SFWM) in a photonic crystal fiber has also been proposed as a source of engineered biphoton states [16,17].

One of the important factors in engineering the frequency-time quantum correlation is the tunability, in that one should be able to move from one type of quantum correlations to another without significantly altering the experimental setup. Such tunable manipulation of frequency-time quantum correlation has been demonstrated with broadband SPDC biphotons by manipulating the spatial profile [18] and the angular dispersion [19] of the pumping laser. Since the medium properties are rather fixed with SPDC, flexible control is generally not possible. Also,

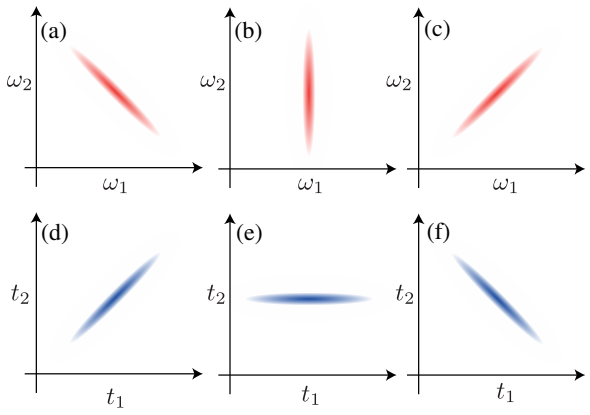

FIG. 1 (color online). Different types of biphoton frequency-time quantum correlations. The joint spectral intensity plots for (a) frequency-anticorrelated, (b) frequency-uncorrelated, and (c) frequency-correlated biphoton states. Because of the Fourier duality, the correlations are reversed in sign in the time domain. For instance, biphotons with frequency anticorrelation in (a) correspond to positive correlation in the joint temporal intensity plot in (d).

such techniques are not applicable to narrow-band entangled photon sources.

In this Letter, we report complete control of frequency-time quantum correlations of narrow-band biphotons, which are generated via the SFWM process based on electromagnetically induced transparency (EIT) in a cold atomic ensemble [20–23]. In our approach, the quantum correlation is tailored by directly manipulating the dispersive property of the cold atomic ensemble (i.e., the EIT medium), hence, controlling the group velocities of the photons involved in the SFWM process. This allows us to generate frequency-anticorrelated, frequency-uncorrelated, and frequency-correlated biphoton states in one experimental setup. Furthermore, Our engineering method with narrow-band SFWM photons will promote various long-distance quantum information applications for their compatibility with atomic quantum memories [24–27].

The experimental scheme is depicted in Fig. 2(a). A cold atomic cloud of 87Rb was prepared in a magneto-optical trap (MOT). During the 10 ms experiment cycle, 9 ms was used for preparing the cold atom cloud and 1 ms was used for the SFWM biphoton generation [28]. The SFWM process in the atomic ensemble generates a pair of quantum correlated Stokes (ω_s) and anti-Stokes ($\omega_{\rm as}$) photons in the presence of the circularly polarized pump (ω_p) and coupling (ω_c) fields. The Stokes (anti-Stokes) biphotons are collected at 3° from the pump (coupling) beams. The single-photon detection events at the detectors $D1$ and $D2$ (Perkin Elmer SPCM-AQRH-13FC) were recorded by using a time-tagging module (SensL HRM-TDC). The joint temporal intensity (JTI) was obtained by integrating the joint detection events for the duration of the pump pulse which was synchronized to the time-tagging module. The JTI due to accidental coincidence events was obtained by measuring pair detection events of Stokes and anti-Stokes photons coming from different pump pulses. The atomic four-level double Λ system used for the SFWM process is described in Figs. 2(b) and 2(c). Here, $|1\rangle \equiv |5S_{1/2}(F=1)\rangle$, $|2\rangle \equiv |5S_{1/2}(F=2)\rangle$, $|3\rangle \equiv |5P_{1/2}(F'=2)\rangle$, $|4\rangle \equiv |5P_{3/2}(F'=2)\rangle$, and, initially, all atoms are prepared in $|1\rangle$. The frequency-anticorrelated and frequency-uncorrelated biphotons are generated with the nondegenerate SFWM scheme shown in Fig. 2(b). The pulsed pump laser is σ^- polarized and the σ^+ polarized cw coupling laser with the diameter of 2.65 mm, resonant with the $|2\rangle \rightarrow |3\rangle$ transition, opens the EIT transparency window for anti-Stokes photons. For the generation of frequency-correlated photon pairs, we adopt the degenerate SFWM scheme shown in Fig. 2(c). Here, both pump and coupling lasers are σ^+ polarized so that Stokes and anti-Stokes photons are identical in polarization as well. Therefore, both Stokes and anti-Stokes photons experience the same EIT slow light effect, controlled by the Rabi frequency of the coupling field.

Unlike SPDC biphotons in which spectral bandwidths are sufficiently large for direct joint spectral intensity

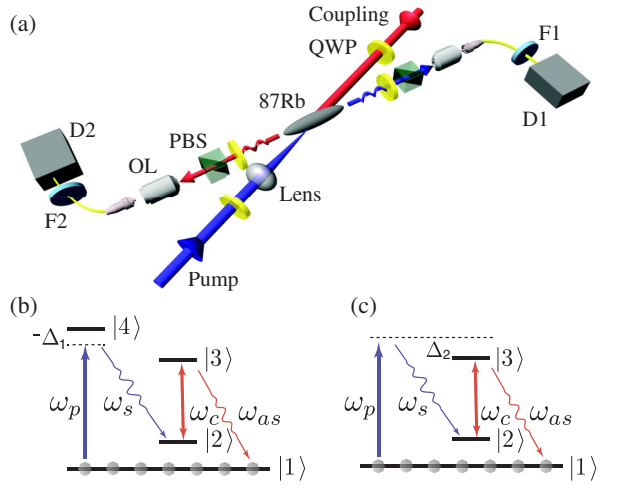

FIG. 2 (color online). Schematic of the experimental setup. (a) An ultracold Rb 87 cloud is prepared in a MOT. The pump (ω_p) and the coupling (ω_c) lasers create a pair of Stokes (ω_s) and anti-Stokes ($\omega_{\rm as}$) photons via the SFWM process. Each photon is collected into a single mode optical fiber with an objective lens (OL) after polarization filtering with a quarter-wave plate (QWP) and a polarization beam splitter (PBS). To block the strong pump and coupling fields, a solid etalon (F1 and F2) with the full width and half maximum (FWHM) bandwidth of 470 MHz is placed in front of each detector ($D1$ and $D2$). (b) SFWM scheme for frequency-anticorrelated and frequency-uncorrelated biphotons. The weak pump is red detuned $\Delta_1 = 2\pi \times 63$ MHz below the $|1\rangle \rightarrow |4\rangle$ transition (peak power: 75 μW). (c) SFWM scheme for frequency-correlated biphotons The strong pump is largely blue detuned $\Delta_2 = 2\pi \times 6.834$ GHz above the $|1\rangle \rightarrow |3\rangle$ so that the Stokes and anti-Stokes photons are frequency degenerate (peak power: 90 mW).

measurement [13], SFWM biphotons from cold atoms are narrow band, so frequency-resolved joint measurement is not practical. Instead, we carry out the JTI measurement for the narrow-band biphotons, as depicted in Figs. 1(d), 1(e), and 1(f). First, let us discuss the nondegenerate scheme in Fig. 2(b). The probability amplitude $A_{s,\rm as}(t_1, t_2)$ that the Stokes photon is detected at $D1$ and the anti-Stokes photon is detected at $D2$ is called the joint temporal amplitude (JTA) and it contains all the information about the temporal correlation in the biphoton state. JTI is simply the absolute square of JTA. In the nondegenerate SFWM scheme in Fig. 2(b), only the anti-Stokes photon experiences the EIT slow light effect and the JTA is calculated to be

$$A_{s,\rm as}(t_1, t_2) = C' E_p(t_1) \Pi(t_2 - t_1; 0, \tau_g), \qquad (1)$$

where all constants are grouped in C', $E_p(t)$ is the pump pulse temporal profile, $\Pi(t)$ is the rectangular function, and $\tau_g \simeq 2\gamma_{13}{\rm OD}/(|\Omega_c|^2 + 4\gamma_{12}\gamma_{13})$ is the group delay. Here, γ_{ij} is the dephasing rate of the $|j\rangle \rightarrow |i\rangle$ transition, Ω_c is the Rabi frequency of coupling laser, and OD is the

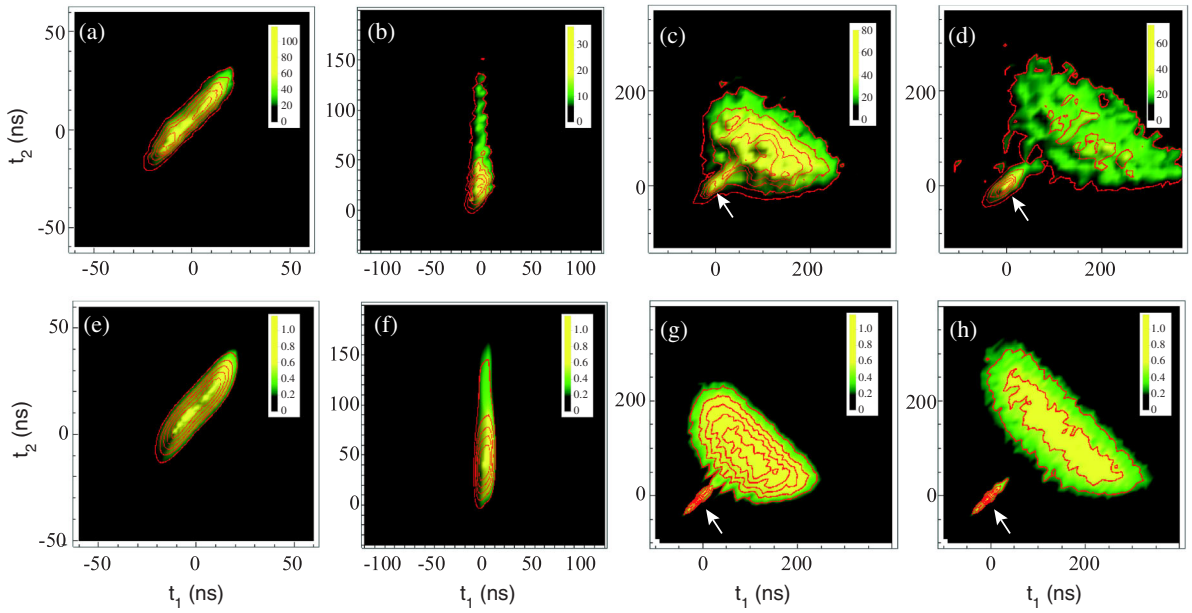

FIG. 3 (color online). Experimental results (a)–(d). Color bars represent coincidence counts. (a) JTI for time-correlated or frequency-anticorrelated biphoton state. Experimental parameters are $\sigma_p = 40$ ns and $\tau_g = 15$ ns (OD = 15, $\gamma_{13} = 2\pi \times 3$ MHz, $\gamma_{12} = 2\pi \times 0.65$ MHz, and $\Omega_c = 2\pi \times 36$ MHz). (b) JTI for time-uncorrelated or frequency-uncorrelated biphoton state. Experimental parameters are $\sigma_p = 20$ ns and $\tau_g = 168$ ns ($\Omega_c = 2\pi \times 10.4$ MHz). (c) JTI for time-anticorrelated or frequency-correlated biphoton state. Experimental parameters are $\sigma_p = 50$ ns and $\tau_g = 178$ ns (OD = 75, $\gamma_{12} = 2\pi \times 0.22$ MHz, and $\Omega_c = 2\pi \times 20$ MHz). (d) JTI for time-anticorrelated or frequency-correlated biphoton state. Here, $\tau_g = 270$ ns ($\Omega_c = 2\pi \times 16.2$ MHz). Arrows in (c) and (d) indicate biphoton optical precursors having positive time correlation. Numerical simulation of JTI (e)–(f). Color bars represent relative intensities. Experimental parameters given in (a)–(d) are used for the simulation (e)–(h), respectively. The JTA of SFWM biphotons is determined by $\chi^{(3)}$ of the medium, the phase matching condition, and pump pulse profile. The numerical simulation also faithfully reproduces the biphoton optical precursor indicated by the arrows in (g) and in (h): see Supplemental Material [29] for the details of the numerical simulation.

optical depth of the cold atom cloud at the $|1\rangle \rightarrow |3\rangle$ transition. [To derive Eq. (1), we have taken the first order Taylor approximation for wave vectors and assumed that the JTA is mainly determined to the phase matching function.] The JTA exhibits positive correlation if $\Pi(t_2 - t_1; 0, \tau_g)$ is the dominant factor, and this can be achieved by making the temporal width of the pump σ_p much bigger than the group delay τ_g.

The experimental result for the time-correlated biphoton state is shown in Fig. 3(a). The measured JTI clearly exhibits time correlation, meaning that the biphoton state is frequency anticorrelated [see Figs. 1(a) and 1(d)]. To generate the time-uncorrelated (or frequency-uncorrelated) biphoton state, we increase the value of τ_g and decrease σ_p because the degree of temporal correlation between the photons is reduced if the arrival time of the Stokes photon is limited by the width of the pump pulse. In experiment, we set the pump pulse width to $\sigma_p = 20$ ns and increase τ_g to 168 ns by reducing the Rabi frequency of the coupling laser Ω_c. The measured JTI for time-uncorrelated biphoton state is shown in Fig. 3(b), [see Figs. 1(b) and 1(e)].

We now consider the degenerate SFWM scheme in Fig. 2(c) for generating the time-anticorrelated (or frequency-correlated) biphoton state. Since the Stokes and anti-Stokes photons are identical, the group velocities in the EIT medium are the same, and the JTA is given as

$$A_{s,\mathrm{as}}(t_1, t_2) = C' E_p\left(\frac{1}{2}(t_1 + t_2 - \tau_g)\right)\Pi(t_2 - t_1; -\tau_g, \tau_g). \tag{2}$$

Here, $E_p[(t_1 + t_2 - \tau_g)/2]$ exhibits negative correlation in time. If $\sigma_p \ll \tau_g$, this term makes the dominant contribution to the JTA, and the overall shape of the JTI will become time anticorrelated, hence, generating the frequency-correlated biphoton state. Note that, in fact, the JTA in the degenerate SFWM scheme is given as a superposition of $A_{s,\mathrm{as}}(t_1, t_2)$ and $A_{\mathrm{as},s}(t_1, t_2)$. In the high OD regime, however, the amplitudes $A_{s,\mathrm{as}}(t_1, t_2)$ and $A_{\mathrm{as},s}(t_1, t_2)$ become nearly identical, so the nature of the frequency-time correlation can be studied with Eq. (2).

In experiment, to ensure that the Stokes and anti-Stokes photons are identical in polarization so as to experience the same polarization dispersion, the pump and coupling lasers are both σ^+ polarized and we detect σ^+ polarized Stokes and anti-Stokes photons. Additionally, in order to match the spectrum of Stokes photons within the EIT bandwidth, the spectral bandwidth of the pump pulse $\sim\sigma_p^{-1}$ should fit

within the EIT bandwidth $\Delta\omega_{\mathrm{EIT}} = \sqrt{\mathrm{OD}}/\tau_g$ [30]. This means that, for a given τ_g, the shorter the pump pulse, the higher the required OD. The experimental results for the time-anticorrelated (or frequency-correlated) biphoton state are shown in Figs. 3(c) and 3(d). The measured JTIs exhibit clear signatures of time anticorrelation [Fig. 1(f)], corresponding to the frequency correlated state [Fig. 1(c)]. We note that higher time anticorrelation can be achieved with higher OD.

It is interesting to observe that, in Figs. 3(c) and 3(d), there are time-correlated JTI peaks near the origin $(t_1, t_2) = (0, 0)$, as indicated by the arrows. These are due to optical precursors of Stokes and anti-Stokes photons, propagating at nearly the vacuum speed of light [31]. While the observation of the optical precursors for a single-photon [32] and for a biphoton [33] have been previously reported, in Figs. 3(c) and 3(d), we report the first time-resolved measurement of the biphoton optical precursor in which the optical precursor is completely separated from the main part of the biphoton. Note that the shape of the optical precursor is independent of Ω_c, affected only by OD [33].

Finally, to confirm that the biphotons are quantum correlated, we measured the joint detection events between Stokes and anti-Stokes photons originating from different pump pulses, obtaining accidental coincidence events. By normalizing the measured JTIs to the maximum accidental coincidence count level, the lower bound for the normalized second-order correlation $g^{(2)}(t_1, t_2)$ is evaluated. Using these values, we evaluated the Cauchy-Schwarz inequality violation factor $\mathcal{R} = [g^{(2)}(t_1, t_2)]^2/[g^{(2)}(t_1, t_1)g^{(2)}(t_2, t_2)]$, where $g^{(2)}(t_1, t_2)$ and $g^{(2)}(t_i, t_i)$ (with $i = 1, 2$) are the normalized second-order cross-correlation and autocorrelation functions, respectively. The results are summarized in Table I. The lower bounds of the experimental $\mathcal{R}$ values clearly indicate that the biphotons are highly quantum correlated, i.e., $\mathcal{R} > 1$. We have also compared the experimentally obtained JTIs in Figs. 3(a)–3(d) with the numerically simulated JTIs in Figs. 3(e)–3(h) by calculating the similarity $\mathcal{S} = \sum_{t_1,t_2} \mathcal{M}_{t_1,t_2}\mathcal{N}_{t_1,t_2}/\sqrt{\sum_{t_1,t_2}\mathcal{M}^2_{t_1,t_2}\sum_{t_1,t_2}\mathcal{N}^2_{t_1,t_2}}$, where $\mathcal{M}_{t_1,t_2}$ and $\mathcal{N}_{t_1,t_2}$ are the discretized theoretical and experimental JTIs, respectively. As summarized in Table I, the experimental JTIs are in good agreement with the numerical simulated JTIs.

TABLE I. Lower bounds of experimental $g^{(2)}(t_1, t_2)$ and $\mathcal{R}$ values. The errors are due to statistical uncertainties of photon counting. All results confirm that the biphotons are strongly quantum correlated. Similarities $\mathcal{S}$ between experimental JTIs in Figs. 3(a)–3(d) and the numerically simulated JTIs in Figs. 3(e)–3(h) show good agreement.

	Fig. 3(a)	Fig. 3(b)	Fig. 3(c)	Fig. 3(d)
$g^{(2)}(t_1, t_2)$	24 ± 2.2	13.3 ± 2.1	10 ± 1.1	10 ± 1.1
$\mathcal{R}$	144 ± 13.2	44.4 ± 6.9	45 ± 2.7	25 ± 2.7
$\mathcal{S}$	0.96	0.89	0.93	0.86

In summary, we have experimentally demonstrated, for the first time, complete control of frequency-time correlations of narrow-band biphotons generated via the spontaneous four-wave mixing process in a cold atomic ensemble. The quantum correlations between the Stokes and anti-Stokes photons are tailored by directly manipulating the dispersive properties of the electromagnetically induced transparency medium. We have experimentally confirmed the generation of frequency-anticorrelated (or time-correlated), frequency-correlated (or time-anticorrelated), and frequency-uncorrelated (or time-uncorrelated) narrow-band biphoton states, as well as verifying strong nonclassicality of the correlations. Our work opens up new possibilities for engineering narrow-band entangled photons for various quantum optical and quantum information applications.

This work was supported in part by the National Research Foundation of Korea (Grants No. 2013R1A2A1A01006029 and No. 2011-0021452). Y.-W. C. and J.-C. L. acknowledge support from the National Junior Research Fellowship (Grants No. 2011-0010895 and No. 2012-000741, respectively). K.-K. P. acknowledges support from the Global Ph.D. Fellowship by the National Research Foundation of Korea (Grant No. 2011-0030856). The authors would like to thank Shengwang Du and Jianming Wen for fruitful discussions.

*Present address: Centre for Quantum Computation and Communication Technology, Department of Quantum Science, The Australian National University, Canberra ACT 0200, Australia.
choyoungwook81@gmail.com
†yoonho72@gmail.com

[1] X.-C. Yao, T.-X. Wang, P. Xu, H. Lu, G.-S. Pan, X.-H. Bao, C.-Z. Peng, C.-Y. Lu, Y.-A. Chen, and J.-W. Pan, Nat. Photonics **6**, 225 (2012).
[2] E. Bimbard, N. Jain, A. MacRae, and A. I. Lvovsky, Nat. Photonics **4**, 243 (2010).
[3] R. Fickler, R. Lapkiewicz, W. N. Plick, M. Krenn, C. Schaeff, S. Ramelow, and A. Zeilinger, Science **338**, 640 (2012).
[4] A. Valencia, G. Scarcelli, and Y. Shih, Appl. Phys. Lett. **85**, 2655 (2004).
[5] V. Giovannetti, S. Lloyd, and L. Maccone, Nature (London) **412**, 417 (2001).
[6] P. J. Mosley, J. S. Lundeen, B. J. Smith, P. Wasylczyk, A. B. U'Ren, C. Silberhorn, and I. A. Walmsley, Phys. Rev. Lett. **100**, 133601 (2008).
[7] P. J. Mosley, J. S. Lundeen, B. J. Smith, and I. A. Walmsley, New J. Phys. **10**, 093011 (2008).
[8] P. G. Evans, R. S. Bennink, W. P. Grice, T. S. Humble, and J. Schaake, Phys. Rev. Lett. **105**, 253601 (2010).
[9] A. Eckstein, A. Christ, P. J. Mosley, and C. Silberhorn, Phys. Rev. Lett. **106**, 013603 (2011).
[10] R. de J. León-Montiel, J. Svozilík, L. J. Salazar-Serrano, and J. P. Torres, New J. Phys. **15**, 053023 (2013).

[11] W. P. Grice, A. B. U'Ren, and I. A. Walmsley, Phys. Rev. A **64**, 063815 (2001).
[12] Y.-H. Kim and W. P. Grice, J. Mod. Opt. **49**, 2309 (2002).
[13] Y.-H. Kim and W. P. Grice, Opt. Lett. **30**, 908 (2005).
[14] O. Kuzucu, F. N. C. Wong, S. Kurimura, and S. Tovstonog, Phys. Rev. Lett. **101**, 153602 (2008).
[15] O. Kuzucu, M. Fiorentino, M. A. Albota, F. N. C. Wong, and F. X. Kärtner, Phys. Rev. Lett. **94**, 083601 (2005).
[16] O. Cohen, J. S. Lundeen, B. J. Smith, G. Puentes, P. J. Mosley, and I. A. Walmsley, Phys. Rev. Lett. **102**, 123603 (2009).
[17] M. Halder, J. Fulconis, B. Cemlyn, A. Clark, C. Xiong, W. J. Wadsworth, and J. G. Rarity, Opt. Express **17**, 4670 (2009).
[18] A. Valencia, A. Ceré, X. Shi, G. Molina-Terriza, and Juan P. Torres, Phys. Rev. Lett. **99**, 243601 (2007).
[19] M. Hendrych, M. Micuda, and J. P. Torres, Opt. Lett. **32**, 2339 (2007).
[20] V. Balić, D. A. Braje, P. Kolchin, G. Y. Yin, and S. E. Harris, Phys. Rev. Lett. **94**, 183601 (2005).
[21] S. Du, P. Kolchin, C. Belthangady, G. Y. Yin, and S. E. Harris, Phys. Rev. Lett. **100**, 183603 (2008).
[22] B. Srivathsan, G. K. Gulati, B. Chng, G. Maslennikov, D. Matsukevich, and C. Kurtsiefer, Phys. Rev. Lett. **111**, 123602 (2013).
[23] S. Yun, J. Wen, P. Xu, M. Xiao, and S.-N. Zhu, Phys. Rev. A **82**, 063830 (2010).
[24] H. Zhang *et al.*, Nat. Photonics **5**, 628 (2011).
[25] B. M. Sparkes, M. Hosseini, C. Cairns, D. Higginbottom, G. T. Campbell, P. K. Lam, and B. C. Buchler, Phys. Rev. X **2**, 021011 (2012).
[26] E. Bimbard, R. Boddeda, N. Vitrant, A. Grankin, V. Parigi, J. Stanojevic, A. Ourjoumtsev, and P. Grangier, Phys. Rev. Lett. **112**, 033601 (2014).
[27] A. MacRae, T. Brannan, R. Achal, and A. I. Lvovsky, Phys. Rev. Lett. **109**, 033601 (2012).
[28] Y.-W. Cho, K.-K. Park, J.-C. Lee, and Y.-H. Kim, J. Korean Phys. Soc. **63**, 943 (2013).
[29] See Supplemental Material at http://link.aps.org/supplemental/10.1103/PhysRevLett.113.063602 for detailed analytical and numerical descriptions of JTA.
[30] M. Fleischhauer and M. D. Lukin, Phys. Rev. A **65**, 022314 (2002).
[31] H. Jeong, A. M. C. Dawes, and D. J. Gauthier, Phys. Rev. Lett. **96**, 143901 (2006).
[32] S. Zhang, J. F. Chen, C. Liu, M. M. T. Loy, G. K. L. Wong, and S. Du, Phys. Rev. Lett. **106**, 243602 (2011).
[33] S. Du, C. Belthangady, P. Kolchin, G. Y. Yin, and S. E. Harris, Opt. Lett. **33**, 2149 (2008).